Supporting Information

Unique 3-D Self-Penetrating Co^{II} and Ni^{II} Coordination Frameworks with a New ($4^4.6^{10}.8$) Network Topology

Dong-Sheng Li,*[ac] Feng Fu,[a] Jun Zhao,[a] Ya-Pan Wu,[ac] Miao Du,*[,b] Kun Zou,[a] Wen-Wen Dong [ac] and Yao-Yu Wang*[,c]

[a]*College of Mechanical & Material Engineering, Hubei Key Laboratory of Natural Products Research and Development, China Three Gorges University, Yichang 443002, China*;

[b]*College of Chemistry, Tianjin Key Laboratory of Structure and Performance for Functional Molecule, Tianjin Normal University, Tianjin 300387, China;*

[c]*Key Laboratory of Synthetic and Natural Functional Molecule Chemistry of Ministry of Education, Department of Chemistry, Northwest University, Xi'an 710069, China*

Dalton

* Corresponding authors

E-mail address: lidongsheng1@126.com (D.-S. Li), Tel./Fax: +86-717-6397516

E-mail address: dumiao@public.tpt.tj.cn (M. Du), Tel./Fax: +86-22-23766556

E-mail address: wyaoyu@nwu.edu.cn (Y.-Y. Wang), Tel./Fax: +86-29-88303798

Materials and General Methods

All the solvents and reagents for syntheses were commercially available and used as received. The FT-IR spectra were recorded as KBr pellets on a Thermo Nicolet Nexus 670 FTIR spectrometer. Elemental analyses were performed on a Perkin-Elmer 2400 Series II analyzer. Powder X-ray diffraction (PXRD) patterns were taken on a Rigaku D/max-2500 diffractometer for Cu Kα radiation (λ = 1.5406 Å), with a scan speed of 2 °/min and a step size of 0.02° in 2θ. The calculated PXRD patterns were obtained from the single-crystal X-ray diffraction data. TG analyses were recorded with a NETZSCH STA 449C microanalyzer under nitrogen at a heating rate of 10 ºC·min^{-1}. Variable-temperature magnetic susceptibilities were measured using a MPMS-7 SQUID magnetometer. Diamagnetic corrections were made with Pascal's constants for all constituent atoms.

Crystallographic Data Collection and Refinement

Single-crystal X-ray diffraction data for complexes **1** and **2** were collected on a Bruker APEX II CCD diffractometer with graphite monochromated Mo Ka radiation (0.71073Å) at 293(2) K. Empirical absorption corrections were applied by using the SADABS program.[1] The structures were solved by direct methods and refined based on F^2 by the full matrix least-squares methods using SHELXTL.[2,3] All non-hydrogen atoms were refined anisotropically, and the H atoms were generated geometrically and refined as riding. Selected bond lengths and angles are listed in Table S1.

References

1 Sheldrick, G M. SADABS, *Program for Empirical Absorption Correction of Area Detector Data*, University of Gottingen, Germany, 1997.

2 Sheldrick, G. M. SHELXS-97, *Program for the Solution of Crystal Structures*; University of Göttingen, Germany, 1997.

3 Sheldrick, G. M. SHELXL, *Program for the Refinement of Crystal Structures*, University of Gottingen, Germany, 1997.

Table S1 Selected Bond Distances (Å) and Angles (deg) for **1** and **2**

1		**2**	
Ni(1)–N(2)	2.140(8)	Co(1)–O(5)#1	2.060(2)
Ni(1)–O(5)#3	2.051(5)	Co(1)–O(6)#2	2.073(3)
Ni(1)–O(6)#2	2.034(5)	Co(1)–O(1)	2.100(2)
Ni(1)–O(1)	2.082(5)	Co(1)–O(7)	2.1593(16)
Ni(1)–O(7)	2.095(4)	Co(1)–N(1)#3	2.177(3)
Ni(1)–N(1) #1	2.221(6)	Co(1)–N(2)	2.187(3)
O(5)#3–Ni(1)–O(6)#2	95.68(19)	O(5)#1–Co(1)–O(6)#2	96.67(9)
O(5)#3–Ni(1)–O(1)	173.5(2)	O(5)#1–Co(1)–O(1)	172.54(9)
O(6)#2–Ni(1)–O(1)	89.40(2)	O(6)#2–Co(1)–O(1)	90.12(9)
O(5)#3–Ni(1)–O(7)	95.21(18)	(5)#1–Co(1)–O(7)	95.04(8)
O(6)#2–Ni(1)–O(7)	85.66(16)	O(6)#2–Co(1)–O(7)	84.80(7)
O(1)–Ni(1)–O(7)	89.16(19)	O(1)–Co(1)–O(7)	88.62(8)
O(5)#3–Ni(1)–N(2)	86.50(3)	O(5)#1–Co(1)–N(1)#3	86.85(10)
O(6)#2–Ni(1)–N(2)	84.10(2)	O(6)#2–Co(1)–N(1)#3	176.26(10)
O(1)–Ni(1)–N(2)	90.00(3)	O(1)–Co(1)–N(1)#3	86.29(10)
O(7)–Ni(1)–N(2)	169.70(2)	O(7)–Co(1)–N(1)#3	96.12(8)
O(5)#3–Ni(1)–N(1)#1	83.80(3)	O(5)#1–Co(1)–N(2)	87.29(9)
O(6)#2–Ni(1)–N(1)#1	177.10(3)	O(6)#2–Co(1)–N(2)	87.22(10)
O(1)–Ni(1)–N(1)#1	90.90(3)	O(1)–Co(1)–N(2)	89.99(9)
O(7)–Ni(1)–N(1)#1	97.20(3)	O(7)–Co(1)–N(2)	171.90(8)
N(2)–Ni(1)–N(1)#1	93.00(3)	N(1)#3–Co(1)–N(2)	91.76(10)

Symmetry codes for **1**: #1 -x-1/2,-y+1/2,-z+1 ; #2 x+1/4,-y+1/2,z-1/4 ; #3 -x,y-1/4,z-1/4; for **2**: #1 -x, y-1/4,z-1/4; #2 x+1/4,-y+1/2,z-1/4; #3 -x-1/2,-y+1/2,-z+1

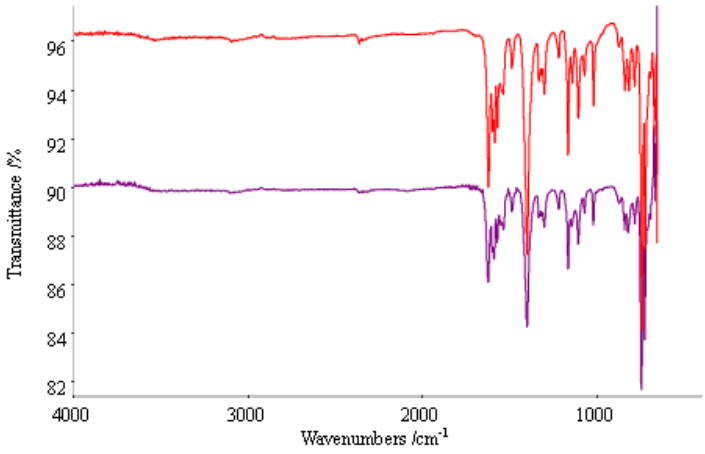

Figure S1a. IR spectra for **1** (red) and **2** (purple).

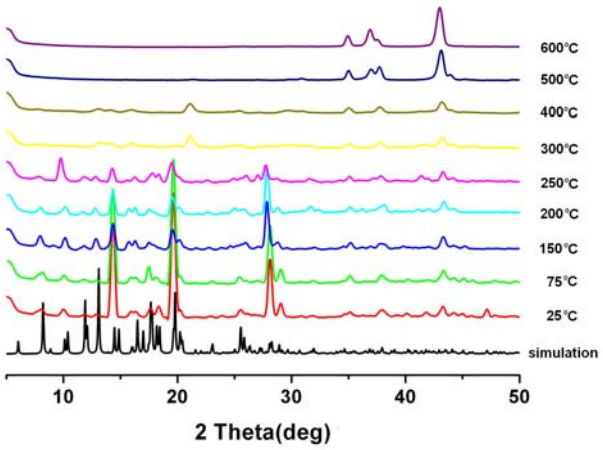

Figure S1b. Temperature-variable PXRD patterns for **1**.

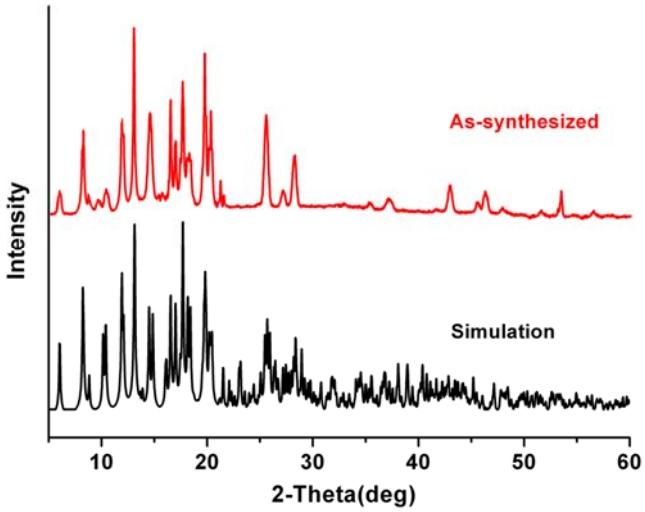

Figure S1c. Simulated and experimental PXRD patterns for **1**.

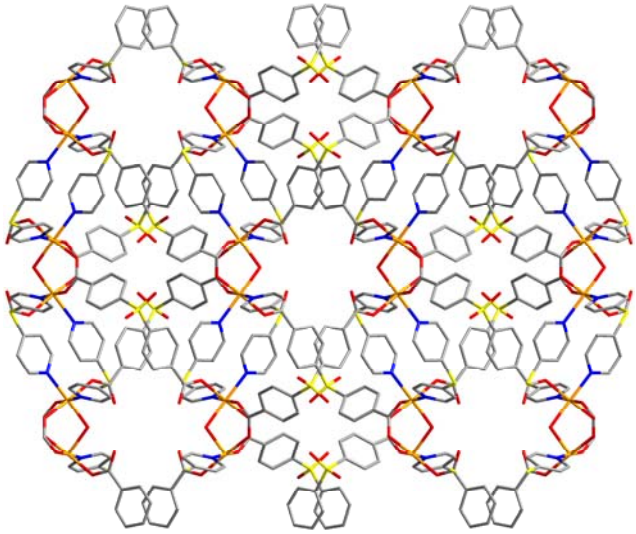

Figure S2. 3-D coordination network with 1-D channel of **1**.

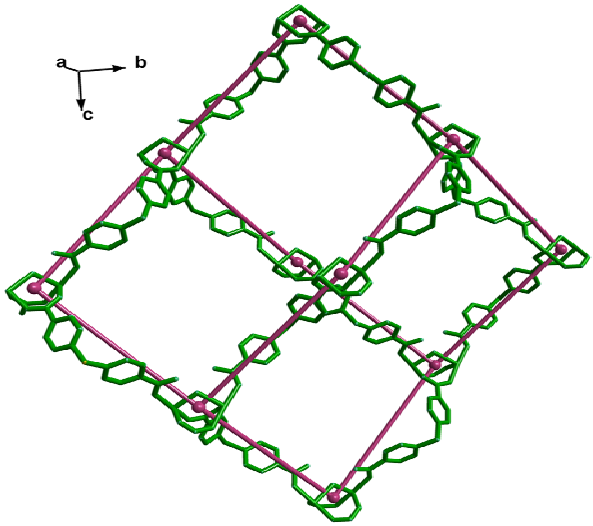

Figure S3a. Single diamondoid cages in each net of **1**.

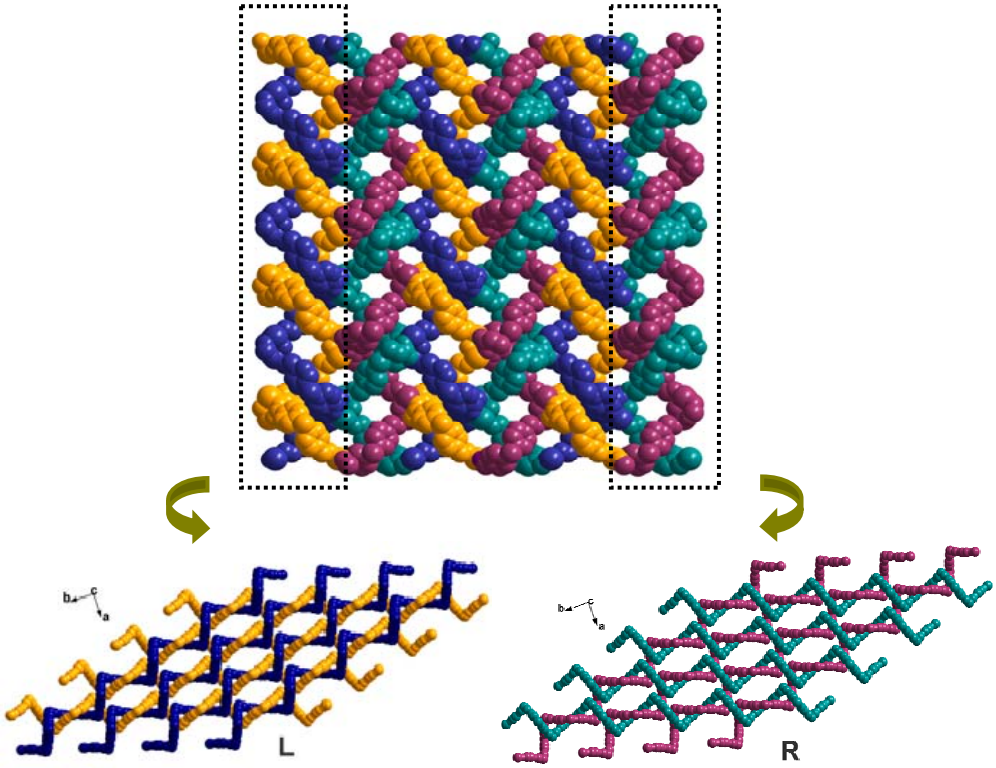

Figure S3b. Two **dia** networks building from "warp and weft" type 2-D networks in an alternate fashion.

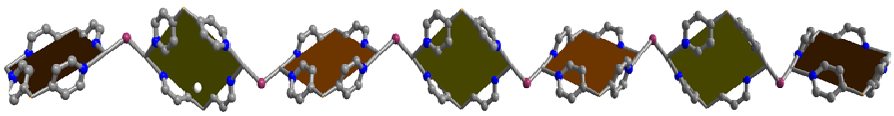

Figure S3c. 1-D quadrate loops constructed from the neighboring dimeric Ni^{II} SBUs and V-shaped dps ligands.

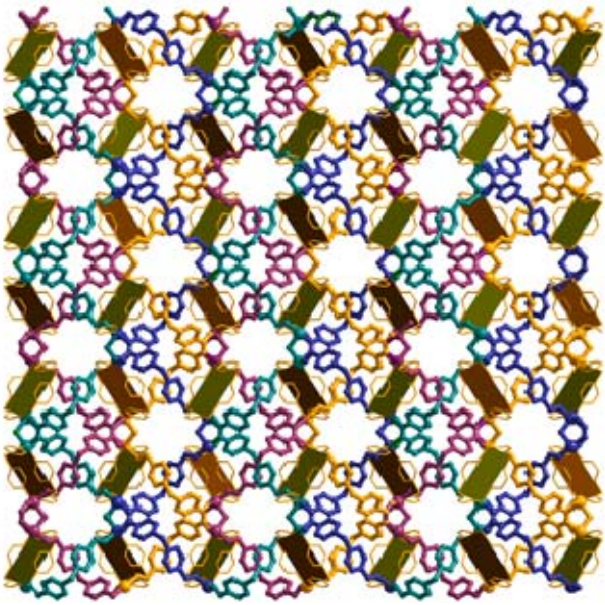

Figure S3d. The final self-penetrating pattern constructed from two **dia** networks and 1-D quadrate loops.

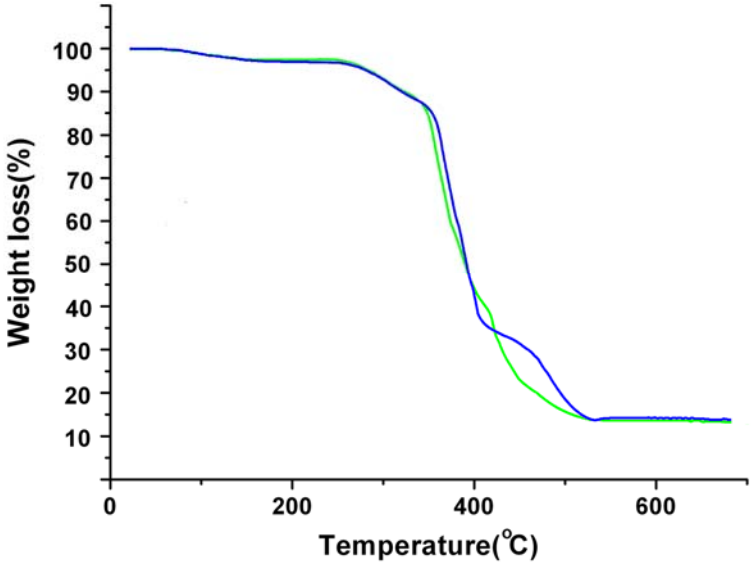

Figure S4. TGA curves of **1** (green) and **2** (blue).